Kontrolle rauschinduzierter Oszillationen im Van-der-Pol Modell

Analyt. Näherung der spektralen Leistungsdichte:

Fourier-Trafo der mean-field-glg.

$$\dot{x} = y$$
$$\dot{y} = \tilde{\varepsilon} y - \omega_0^2 x + D\xi(t) + K[y(t-\tau) - y(t)]$$

$$x(t) = \int_{-\infty}^{\infty} d\omega\, e^{-i\omega t}\, \hat{x}(\omega)$$

$$-i\omega \hat{x}(\omega) = \hat{y}(\omega)$$
$$-i\omega \hat{y}(\omega) = \tilde{\varepsilon}\hat{y}(\omega) - \omega_0^2 \hat{x}(\omega) + D\hat{\xi}(\omega) + K\hat{y}\left(e^{i\omega\tau} - 1\right)$$

Elim. von $\hat{x}(\omega) = \frac{i}{\omega}\hat{y}(\omega)$:

$$-i\omega\hat{y} - \tilde{\varepsilon}\hat{y} + i\frac{\omega_0^2}{\omega}\hat{y} - K\left(e^{i\omega\tau} - 1\right)\hat{y} = D\hat{\xi} \qquad |\cdot i\omega$$

$$\hat{y}(\omega) = \frac{i\omega D\hat{\xi}(\omega)}{\omega^2 - \omega_0^2 - i\omega\tilde{\varepsilon} - i\omega K\left(e^{i\omega\tau} - 1\right)}$$

$$\langle \hat{y}(\omega)\hat{y}^*(\omega')\rangle = \frac{(i\omega)(-i\omega' D)\langle \hat{\xi}(\omega)\hat{\xi}^*(\omega')\rangle}{\left(\omega^2 - \omega_0^2 - i\omega\left[\tilde{\varepsilon} + K\left(e^{i\omega\tau} - 1\right)\right]\right)\left(\omega'^2 - \omega_0^2 + i\omega'\left[\tilde{\varepsilon} + K\left(e^{-i\omega'\tau} - 1\right)\right]\right)}$$

$$\langle \hat{\xi}(\omega)\hat{\xi}^*(\omega')\rangle = \frac{1}{(2\pi)^2}\int_{-\infty}^{\infty} dt\, e^{i\omega t}\int_{-\infty}^{\infty} dt'\, e^{-i\omega' t'}\underbrace{\langle \xi(t)\xi(t')\rangle}_{\delta(t-t')}$$

$$= \frac{1}{2\pi}\underbrace{\frac{1}{2\pi}\int_{-\infty}^{\infty} dt\, e^{i(\omega-\omega')t}}_{\delta(\omega-\omega')}$$

$$\omega = \omega' \Rightarrow \langle \hat{y}(\omega)\hat{y}^*(\omega')\rangle = \frac{D^2}{2\pi}\frac{\omega^2\,\delta(\omega-\omega')}{\left(\omega^2 - \omega_0^2 + \omega K\sin\omega\tau\right)^2 + \omega^2\left(\tilde{\varepsilon} - K(1-\cos\omega\tau)^2\right)}$$

Wiener-Khinchine-Theorem:

$$\langle \hat{y}(\omega)\hat{y}^*(\omega')\rangle = \frac{1}{(2\pi)^2}\int_{-\infty}^{\infty} dt\, e^{i\omega t}\int_{-\infty}^{\infty} dt'\, e^{-i\omega' t'}\langle y(t)y(t')\rangle \qquad t+s$$

$$= \underbrace{\frac{1}{2\pi}\int_{-\infty}^{\infty} dt\, e^{i(\omega-\omega')t}}_{\delta(\omega-\omega')}\ \underbrace{\frac{1}{2\pi}\int_{-\infty}^{\infty} ds\, e^{i\omega'(t-t')}\langle y(t)y(t+s)\rangle}_{S(\omega')} \qquad -s$$

$$\Rightarrow S_{yy}(\omega) = \frac{D^2}{2\pi}\,\frac{\omega^2}{(\omega^2-\omega_0^2+\omega K\sin\omega\tau)^2+\omega^2(\tilde{\varepsilon}-K(1-\cos\omega\tau))^2}$$

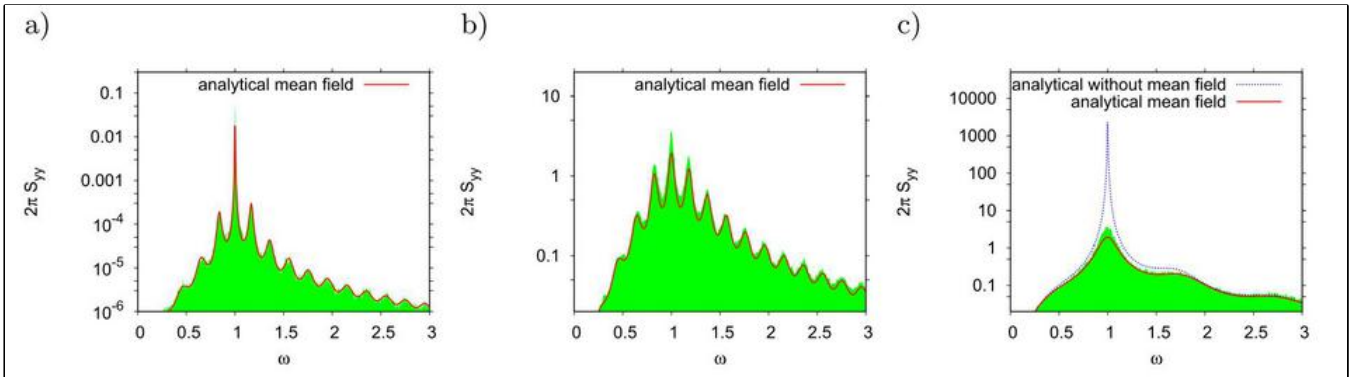

Fig. 4 – Spectrum $S_{yy}(\omega)$ for the VdP system in the presence of delayed feedback for $\varepsilon = -0.01$, $K = 0.2$: a) $D = 0.003$, $\tau = 31.4$; b) $D = 0.5$, $\tau = 31.4$; c) $D = 0.5$, $\tau = 6.3$. Shaded: numerically simulated spectra; solid line: spectrum estimated analytically by (19); dashed line in c): spectrum estimated analytically without mean field ($\tilde{\varepsilon} = \varepsilon$) [14].

Pompium et al, Europhys. Lett. 2005

bemerkenswerte Übereinstimmung der mean-field-Näherung mit der vollen nichtlin. Simul. der Dgl., sogar für große D

$K=0$: $S(\omega) = \frac{D^2}{2\pi}\,\frac{\omega^2}{(\omega^2-\omega_0^2)^2+\omega^2\tilde{\varepsilon}^2}$

Lorentzkurve mit Max. bei ω_0 u. Halbwertsbreite $\approx \frac{|\tilde{\varepsilon}|^2}{2} = \frac{2}{\pi t_{cor}}$

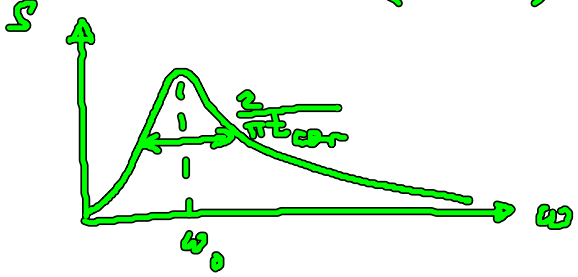

$K \neq 0$: immer mehr Nebenmax. mit zunehmendem τ

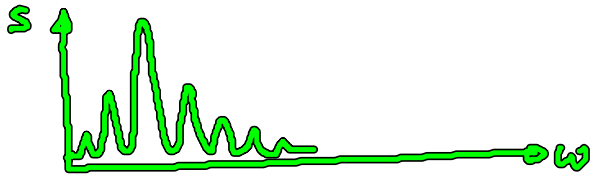

generisches Modell für Anregbarkeit Typ I

(knapp unterhalb der SNIPER-Bifurkation)

Aust, Hövel, Hizanidis, Schöll, Eur. Phys. J. - ST 187, 77 (2010)

$$\dot{x} = x(1-x^2-y^2) + y(x-b) + D\xi(t) + K[x(t-\tau) - x(t)]$$
$$\dot{y} = y(1-x^2-y^2) - x(x-b) + D\xi(t) + K[y(t-\tau) - y(t)]$$

$K = D = 0$

$b < 1$: stab. Fixp. (Knoten), anregbares Regime

$b = 1$: Sattel-Knoten-Bif. auf Grenzzyklus $r = 1$, $T \to \infty$

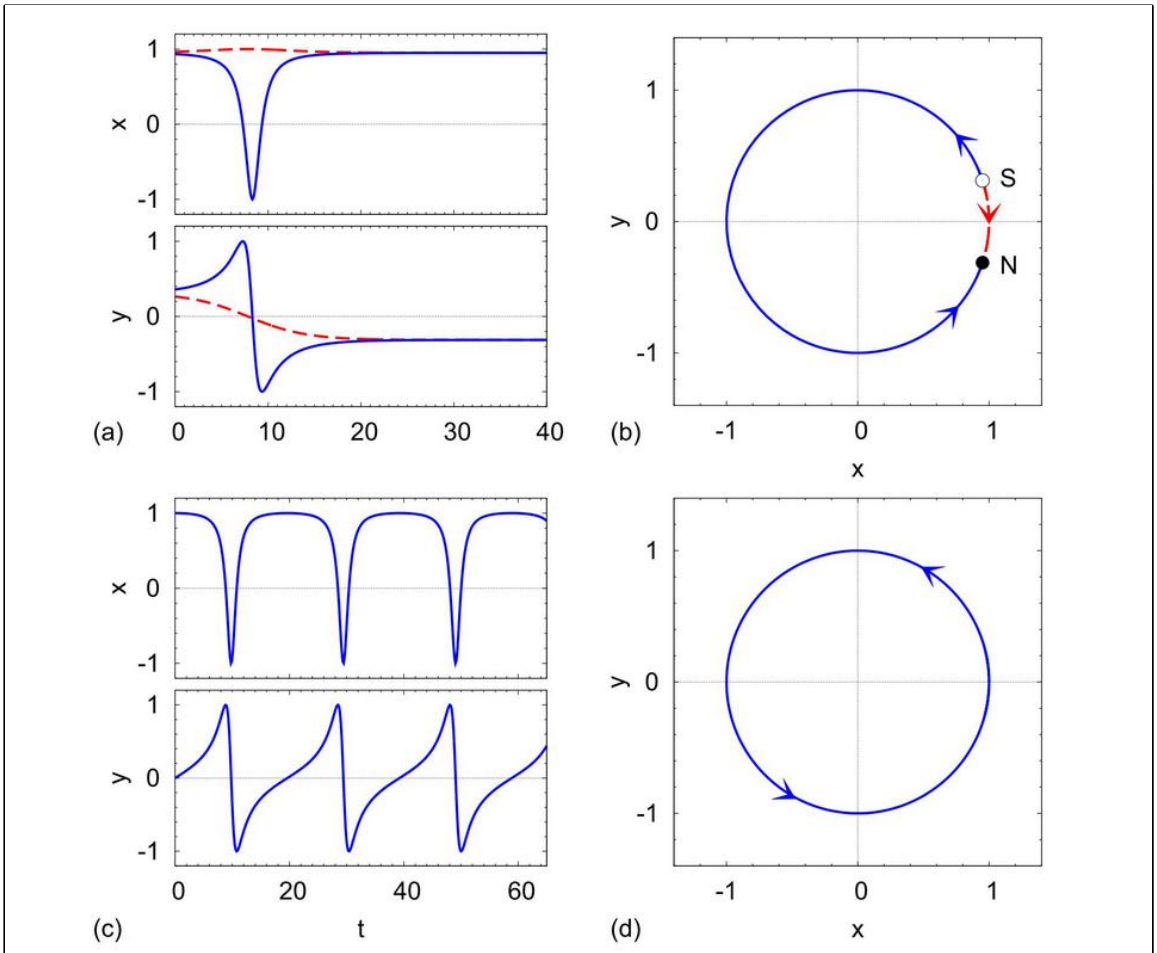

Fig. 1. (Color online) Time series (a),(c) and phase portraits (b),(d) of the analytic solutions of Eqs. (2). Panels (a),(b) refer to $b = 0.95 < 1$ with analytic solutions given by Eq. (7); full (blue) and broken (red) lines refer to two different initial conditions. Panels (c),(d) correspond to $b = 1.05 > 1$, see Eq. (8). ($K = D = 0$)

$D = 0$: Delay-induzierte globale (homokline) Bifurk.

Hizanidis et al., Int. J. Bif. Chaos 18, 1759 (2008)

Fixp. N (node) bleibt stabil, aber homokline Bif. eines stab. Grenzzyklus $r > 0$, $T \to \infty$

im Bif. pkt.

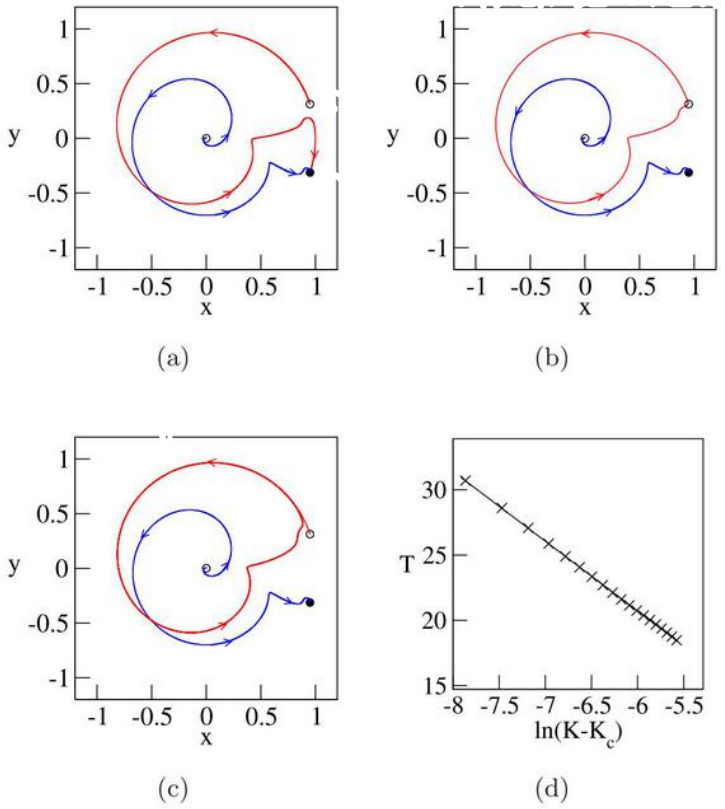

Fig. 2. (a) Two-dimensional projection of the phase space below the homoclinic bifurcation ($K = 0.335$). (b) Homoclinic orbit (red) achieved at $K_c = 0.3401$. (c) Delay-induced limit cycle (red) above the homoclinic bifurcation ($K = 0.3438$). (d) Scaling of the oscillation period T above but close to the critical point K_c (crosses: simulation data, solid line: linear fit). Full and open circles mark stable and unstable fixed points, respectively. Parameters: $b = 0.95$, $\tau = 3$.

Periode $T \sim \ln|K - K_c|$

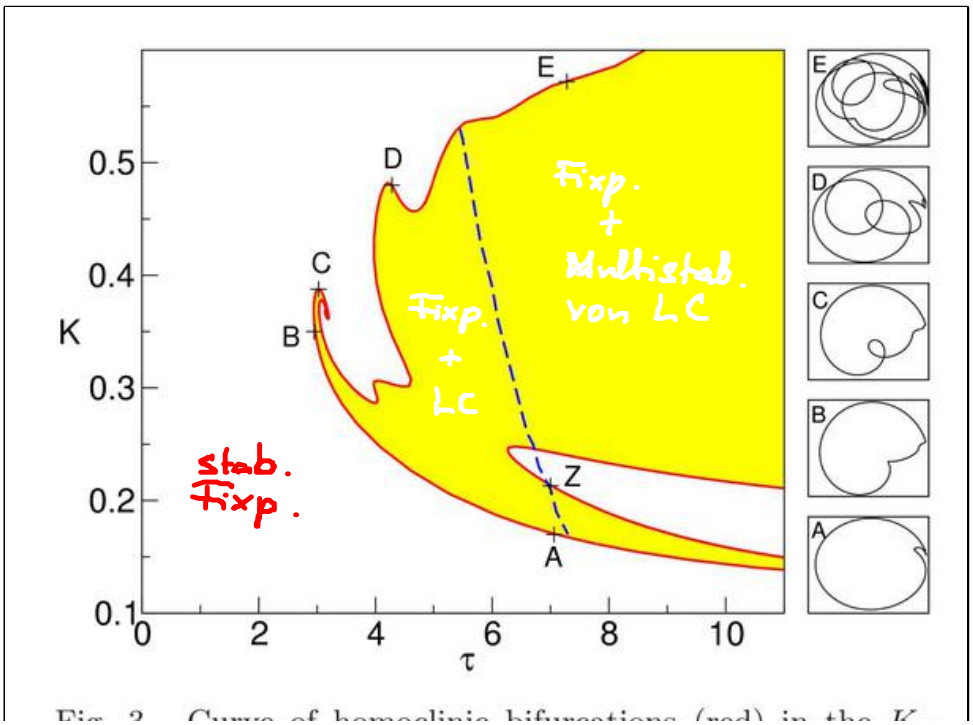

Bif. diagramm (D=0)

Shilnikov-Theorie
saddle quantity
$\sigma_0 = \mathrm{Re}\,\Lambda_s + \mathrm{Re}\,\Lambda_u$

Fig. 3. Curve of homoclinic bifurcations (red) in the K–τ plane (left). A–E labels various points with homoclinic orbits, which are shown in the x–y phase plane in the panel on the right. Delay-induced limit cycles exist, in addition to the stable fixed point, in the yellow area. The blue dashed curve separates the regions $\sigma_0 < 0$ (left) and $\sigma_0 > 0$ (right).

führende stab./instab. Eigenwert des Sattel-Fokus

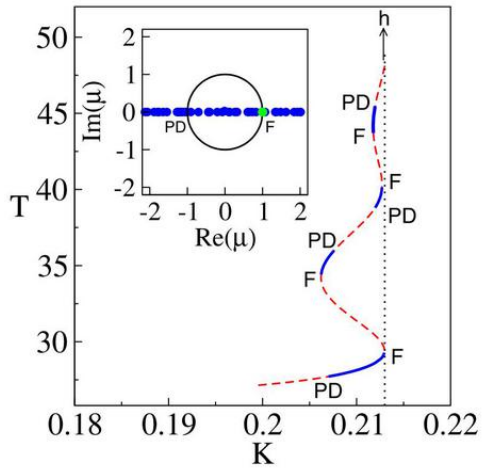

(b)

Fig. 5. (a) Period T of limit cycle born in a homoclinic bifurcation at $(K, \tau) = (0.17145, 7)$ (point A in Fig. 3, $\sigma_0 < 0$). (b) Period T of limit cycles in the multistable regime at $(K, \tau) = (0.213, 7)$ (point Z in Fig. 3, $\sigma_0 > 0$), undergoing infinitely many fold (F) and period-doubling (PD) bifurcations, before ending in a homoclinic orbit h for $T \to \infty$ at $K = 0.213$. Solid blue and red dashed lines denote stable and unstable limit cycles, respectively. The insets show the two leading Floquet multipliers of the periodic orbit $\mu_1 = 1$ (green) and μ_2 (blue) with K as a parameter in (a), and T as a parameter in (b), in the complex plane $b = 0.95$.

$D \neq 0$: Kontrolle rauschinduzierter + rauschbeeinflusster Oszillationen

delay-induzierte deterministische Grenzzyklen

- Kohärenzresonanz (für $K = 0$) wird verstärkt durch zeitverzögerte Rückkopplungskontrolle

Anst et al (2010)

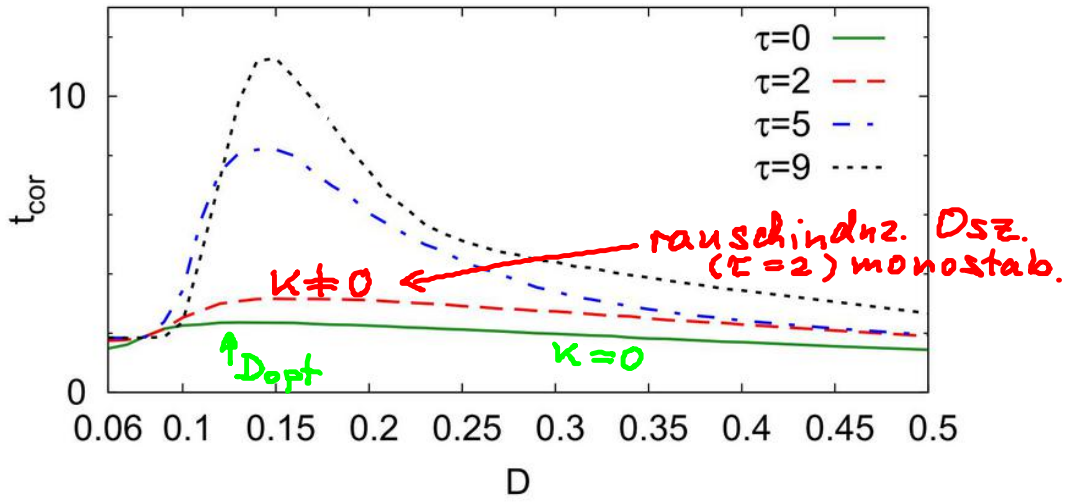

Fig. 4. (Color online) Correlation time in dependence on the noise intensity D for different time delays τ. The solid (green) curve corresponds to the uncontrolled system ($\tau = 0$). The dashed (red), dash-dotted (blue), and dotted (black) curves refer to values of $\tau = 2, 5$, and 9, respectively. Other parameters: $b = 0.95$ and $K = 0.25$.

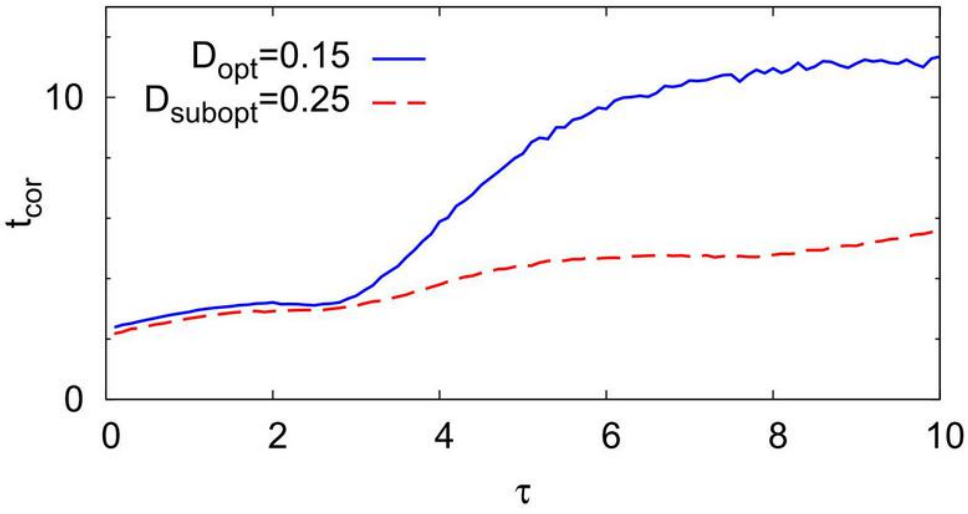

Fig. 5. (Color online) Correlation time t_{cor} in dependence on the time delay τ for two values of the noise intensity D. The dashed (red) curve corresponds to $D_{subopt} = 0.25$ and the solid (blue) curve refers to $D_{opt} = 0.15$. Other parameters: $b = 0.95$ and $K = 0.25$.

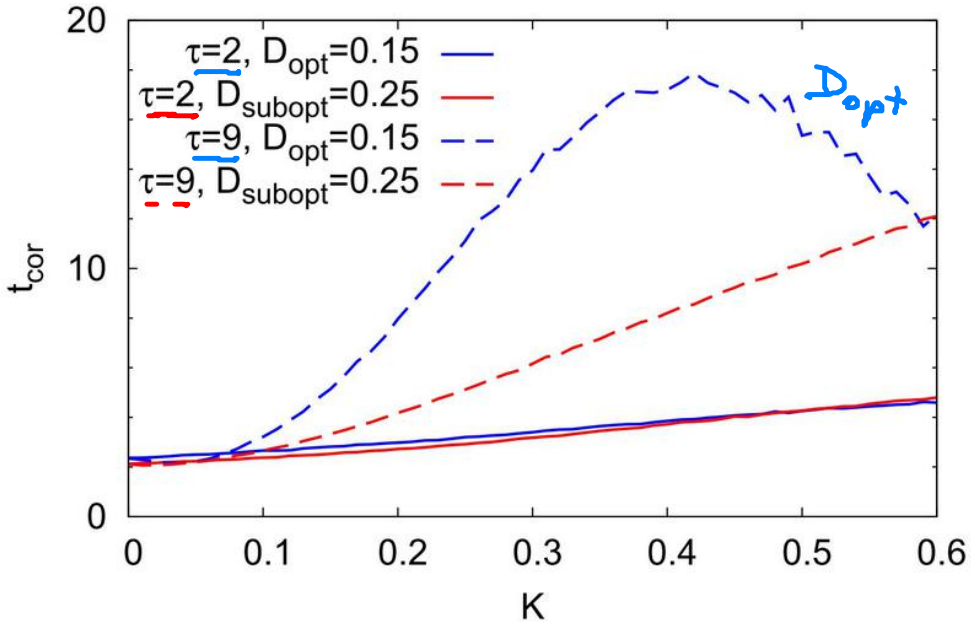

Fig. 6. (Color online) Correlation time t_{cor} in dependence on the control strength K for two values of the noise intensity D and two values of the delay time τ. The gray (red) and black (blue) curves depict the cases of D_{subopt} and D_{opt}, respectively. The solid and dashed lines correspond to $\tau = 2$ and $\tau = 9$, respectively. Other parameter: $b = 0.95$.